A Plus-shaped Slot MIMO Antenna with High Reduction Coupling via Hybrid Isolation Technique

Mohammed S. Al Ani, Ahmed Raed Al-Tameemi, Goh Chin Hock, Tiong Sieh Kiong, Taha Raad Al-Shaikhli, and Mudhafar Fadhil

Original scientific article

***Abstract*—A compact multi-input multi-output (MIMO) antenna for sub-6 GHz 5G communication is proposed in this article. The proposed antenna consists of a plus-shaped slot with a microstrip feed line positioned inside a rectangular patch after etching a circular slot. The antenna elements are placed oppositely with an edge-to-edge spacing of only 4 mm. To reduce mutual coupling, a hybrid isolation technique consisting of two pairs of vertical and horizontal neutralization lines (NLs) combined with a defected ground structure (DGS) is employed. The proposed technique reduces the mutual coupling below −26 dB in the worst-case scenario and achieves a peak isolation of −35 dB over the operating frequency band from 5.17 to 5.47 GHz. The combination of different isolation techniques improves coupling reduction efficiency without increasing the antenna size or inter-element spacing. The final results show an isolation improvement of approximately 14 dB compared to the reference design. The proposed MIMO antenna has compact dimensions of 31 × 31 × 1.6 mm³ and is printed on a low-cost FR-4 substrate. Fabrication and measurement processes were carried out, and the measured results show good agreement with the simulated results. Other antenna performance parameters, including envelope correlation coefficient (ECC), radiation efficiency, and gain, were also investigated. The obtained results demonstrate that the proposed antenna is a suitable candidate for modern sub-6 GHz 5G communication devices.**

***Index terms*—MIMO, isolation, Hybrid isolation technique, mutual coupling reduction.**

I. Introduction

Multiple-Input Multiple-Output (MIMO) antenna systems have become foundational to modern wireless communication driving advancements from Wi-Fi and LTE to 5G and beyond through their ability to significantly increase channel capacity and link reliability [1]. However, the increasing of antenna elements, mutual coupling (i.e., unwanted electromagnetic interaction between proximate antenna elements) becomes a critical limiter, degrading parameters such as impedance matching, envelope correlation coefficient (ECC), gain, and overall system performance [2].

Many significant research has been dedicated to developing efficient isolation techniques to suppress mutual coupling and enhance isolation performance in compact MIMO antenna systems and different isolation methods have been explored.

The explored isolation techniques is defected ground structures (DGS) [3], neutralization lines (NL) [4], decoupling networks (DN) [11], parasitic elements (PE) [5], various metamaterial-inspired techniques such as electromagnetic band gap (EBG) structures [7], [8] and hybrid technique [6], [12]. In [3], a four-element rectangular patch MIMO antenna was proposed, where three slots were etched on a separated ground plane (DGS). The achieved results show isolation level of approximately −28 dB. Similarly, in [4], the neutralization line technique was inserted between two L-shaped radiators. The antenna achieved an enhanced isolation ranging from −8 dB to −45 dB over the operational bandwidth. This work [5], proposed a four-element S-shaped radiator antenna to operate at triple bands for sub-6 GHz and mm-wave 5G applications. plus-shaped stubs were printed between the radiators as parasitic elements to enhance isolation. UWB MIMO antenna with EBG structure was presented in [7]. The used EBG structure consists of chain-shaped parasitic structure and T-type slits within the antenna layout. The obtained results show a good enhancement in terms of isolation about −25 dB. Another EBG-based solution was presented in [8], where an S-shaped EBG structure was inserted between square micro-strip patch antennas with G-slots. This design reduced coupling to about −10.5 dB. A hybrid isolation approach was adopted in [6], where a circular monopole MIMO antenna incorporated both DGS and NL techniques. The combined effect of these isolation methods resulted in a coupling reduction from −12 dB to −22 dB. In [11], a coupled resonator decoupling network (CRDN) was proposed for three-element MIMO arrays. This method was based on the synthesis of mutual admittance parameters and provided both matching and decoupling functionality. The results showed substantial coupling suppression below −20 dB. On the other hand, in [12], a neutralization-line-incorporated decoupling network (NLDN) was presented for wideband multi-element arrays. This technique eliminated the need for

Manuscript received October 15, 2025; revised November 7, 2025. Date of publication October 20, 2026. Date of current version October 20, 2026. The associate editor prof. Gordan Šišul has been coordinating the review of this manuscript and approved it for publication.

M. S. Al Ani is with the College of Engineering Technology, Al-Farahidi University, Baghdad, Iraq (e-mail: mr.muhammed.salim@uoalfarahidi.edu.iq).

A. R. Al-Tameemi is with the Department of Computer Engineering, University Technology and Al-Nisour University College, Baghdad, Iraq (e-mail: ahmed.r.mohammed@uotechnology.edu.iq).

G. C. Hock and T. S. Kiong are with the College of Engineering, Universiti Tenaga Nasional, Kajang, Malaysia (e-mails: {chinhock, Siehkiong}@uniten.edu.my).

T. R. Al-Shaikhli is with the Department of Computer Engineering, University Technology and Al-Nisour University College, Baghdad, Iraq (e-mail: taha.r.eng@uotechnology.edu.iq).

M. Fadhil is with the Department of Cybersecurity Engineering, Al-Nisour University College Baghdad, Iraq (e-mail: assim.m.itm@nuc.edu.iq).

Digital Object Identifier (DOI): 10.24138/jcomss-2025-0139

separate matching circuits while effectively enhancing isolation and maintaining compactness. Overall, the literature demonstrates the continuous evolution of isolation techniques in MIMO antenna systems but the most of published works have been used a traditional single isolation technique and the distance between antenna is big these two factors represent the research gap of this study. Therefore, there is a need for explore new hybrid techniques and investigate the engineering structure to study their outcomes.

In this study, a plus-shaped slot MIMO antenna with high isolation below -25 dB and low distance below 10 mm between the radiator elements. The identical elements were located vertically on FR-4 substrate with a thickness of 1.6 mm. A hybrid isolation technique has been used to improve isolation among radiator elements. The proposed hybrid isolation technique consists of NLs printed on the ground plane of the substrate and etching a slot on the ground plane which acts as DGS. The achieved results after this modification show high isolation below -26 dB and peak isolation was -40 dB. Performance of the proposed antenna shows a good agreement with the requirement of Wi-Fi and WLAN of 5G sub-6 GHz.

The main contribution of this study is:

- Designing a compact MIMO antenna with a small distance between elements.
- Employee a hybrid isolation technique of defected ground structure (DGS) and neutralization line (NL) to achieve high isolation to be applicable for 5G systems.

This work is organized as follows: Section II represents research method, design progress, and working mechanism. Section III presents results of applied parametric studies. Section IV presents and discusses the measured results of the fabricated antenna. Section V provides a comparison with related works. Finally, Section VI presents the calculation of this word.

II. Research Method

The basic unit of the proposed antenna is a rectangular patch, developed through a five-stage design process. In the initial stage, a rectangular antenna (Antenna 1) was created with dimensions of 13 × 18 mm². The operating frequency of the patch was determined using Equation (1).

$$f_r = \frac{c}{2L\sqrt{\varepsilon_r}} \quad (1)$$

In the second stage, a circular slot with a radius of R1 = 5.5 mm was introduced. Figure 1 (Ant 2) illustrates antenna 2, which was formed by integrating Ant 1 with the circular slot. In the third stage, another circular patch, R2, with a radius of 4.5 mm is introduced, which is etched to make the four slots and central circular with a radius of 2 mm to create Ant 4. In the final stage, the final antenna (Antenna 5) was developed by merging Ant 2 and Antenna 4, as depicted in Fig 1 (Ant 5).

Next, the proposed antenna consists of two antenna elements printed on opposite sides of an FR-4 substrate with overall dimensions of 31 × 31 × 1.6 mm³. The edge-to-edge spacing between the two antenna elements is 4 mm. A ground plane is printed on the reverse side of each antenna element with dimensions P14 × P12, as illustrated in Figure 2. To achieve high isolation between the antenna elements, neutralization lines (NLs) were implemented between them on the ground plane. These NLs were integrated into a defected ground structure (DGS) formed by etched slots with dimensions P16 and P13. The dimensions of the neutralization lines and the spacing between adjacent NLs are shown in Figure 2(b). The detailed dimensions of the proposed MIMO antenna are listed in Table I.

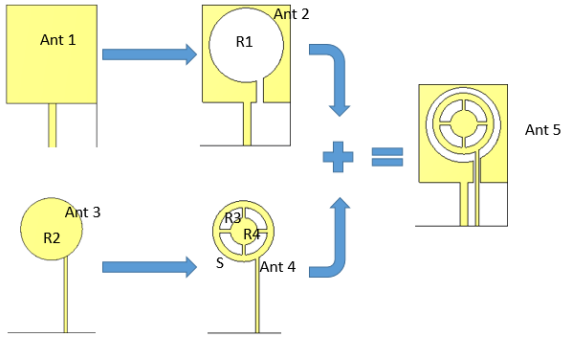
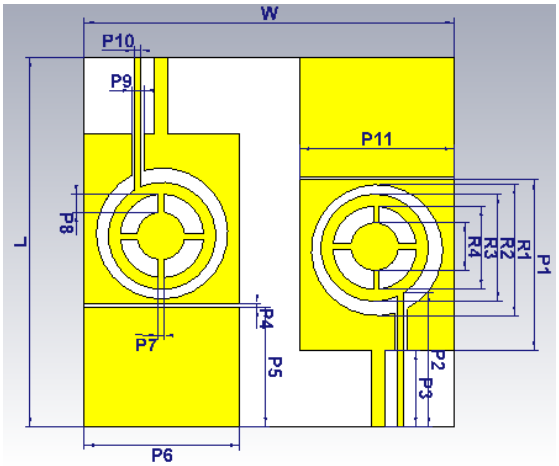
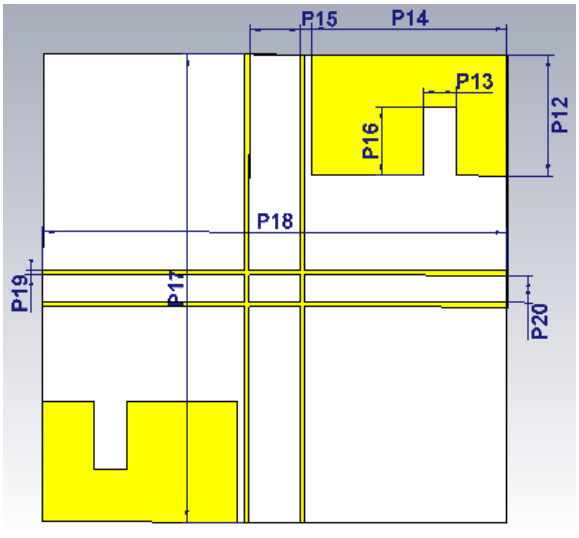


Fig. 1. Evaluation steps of plus-shaped slot MIMO antenna.



(a)



(b)

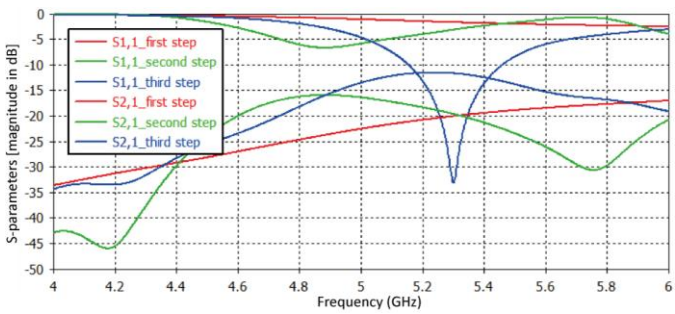
Fig. 2. Proposed MIMO antenna geometry: a) front view, b) back view.

TABLE I
PLUS-SHAPED MIMO ANTENNA DIMENSIONS

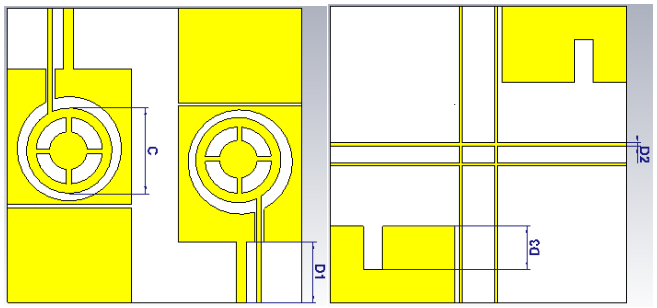
Parameters	Dimensions (mm)	Parameters	Dimensions (mm)
W=L	31	R1	11
R2	9	R3	7
R4	4	P1	14.3
P2	11.23	P3	6.4
P4	0.3	P5	10
P6	13	P7	0.5
P8	1.5	P9	1
P10	0.5	P11	13
P12	8	P13	2.2
P14	13	P15	3.4
P16	4.5	P17=P18	31
P19	0.3	P20	1.8

III. EVALUATION PROGRESS AND PARAMETRIC ANALYSIS

A slot MIMO antenna is proposed in this work with a compact distance between antenna elements of 4 mm. The MIMO antenna consists of two identical elements of circular patch with four etched slots to create a plus-shaped radiator element (first step). A circular plus-shape was surrounded by a traditional rectangle of copper with a circular gap in the inner surface (second step). Finally. A rectangular strip was located up to the traditional rectangle with a gap of 0.3 mm to make a controller of operating frequency. In all three design steps the dimension of the ground plane was 13 × 8 mm^2. The s-parameter results of the three steps mentioned above are demonstrated in Fig. 3. The red curve of figure 3 represented the first step; it can find that there is no frequency resonance in this step. The green curve illustrates the second step of MIMO antenna design. It's notable that the antenna's impedance matching improved and it resonated at 4.8 GHz (operation frequency below -6); otherwise, the coupling between antennas below -15 dB, as seen in the green curve in figure 3. In the final step, after adding the rectangular strips up the radiator elements. The blue curve illustrates the results of this step; it can be noted that the antenna operating frequency is shifted toward operating at 5.3 GHz with improved matching impedance below -33 dB, while the coupling between antennas increased to be below -11 dB. Figure 3(b) demonstrate the main dimension which will be in the parametric study to enhance the MIMO antenna performance.



(a)



(b)

Fig. 3. Proposed MIMO antenna: a) S-parameters of MIMO antenna evaluation, b) parameters considered in the parametric study.

Different parametric values were applied on value of C (represent P5) to investigate the effects on the s-parameters depending on the CST software system while the used port was lumped port boundary conditions to emulate free-space conditions while the simulation carried by out using the frequency-domain solver. Figure 4 demonstrate the s-parameters of changing value from 4.5 to 4.7 mm with a step of 0.1 mm. It can be released that the antenna has a resonance frequency at 5.3 GHz with peak matching of -34.1 dB and an operating frequency bandwidth from 5.15 to 5.48 GHz when C= 4.5 mm. While when C = 4.6 mm, the operating frequency slightly reduced to be operated at 5.28 GHz with reduced matching impedance below -30 dB and an operating band of 5.11-5.41 GHz. At the last step of this parametric study, the blue curve shows that the operating frequency antenna again reduced to be operate at 5.2 GHz with a strong reduction in terms of matching impedance below -20 dB. In terms of isolation, it was noted that there is no significant effect through this parametric study. From the achieved result, each time when the value of C was minimized, the operating frequency shifted to a lower frequency. Therefore, we found that the better value of C was 4.5 mm to keep the matching high.

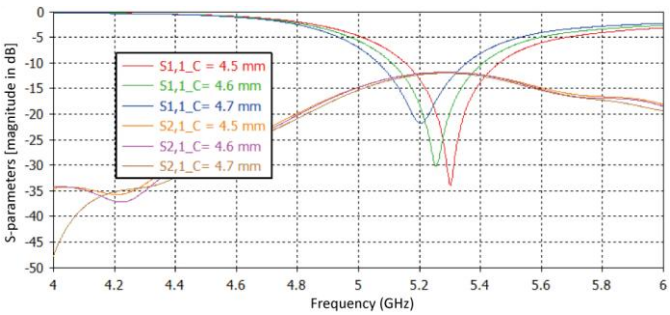
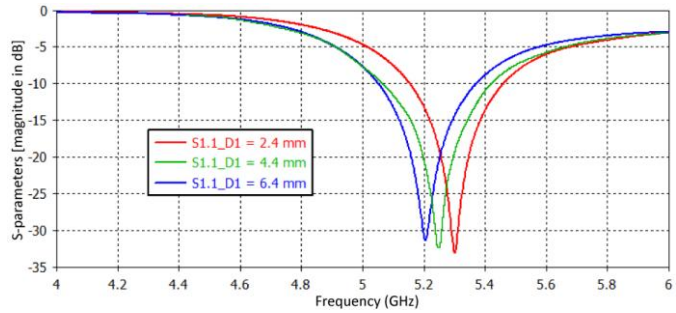


Fig. 4. Main parameters which applied parametric study S-parameters results of changing value of C.

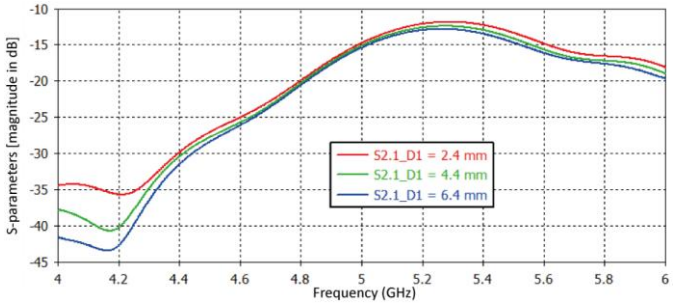
In this step, a strip with dimensions of 2.4 × 1.09 mm² is connected to the square patch, and a parametric study was conducted on the strip length (D1), varying it from 2.4 mm to 6.4 mm in steps of 2 mm. The S-parameter results of this parametric study are presented in Figure 5. The red curve represents S_{11} and S_{21} when D1 = 2.4 mm, showing that the MIMO antenna has no significant effect on S_{11} and S_{21}. However, when D1 is increased to 4.2 mm, the resonance frequency shifts down to 5.27 GHz, with a slight reduction in

impedance matching. At D1 = 6.4 mm, the frequency continues to shift, now resonating at 5.2 GHz, with a further decrease in matching impedance. The coupling between antenna elements is slightly affected in this parametric analysis and enhanced from -11.5 to below -13.5 dB due to the suppression of a part of the electromagnetic energy to transform to adjust the element.

From this study, effectively increases the electrical length of the current path on the patch. This occurs because the surface current is forced to detour around the slot edges, resulting in a longer propagation path. Therefore, the ideal value of D1 is 4.6 mm, as it enables the antenna to operate at the desired frequency.



(a)



(b)

Fig. 5. S-parameter results of changing the length of the loaded strip on the front view: a) S11, b) S21.

Due to the strong coupling between MIMO antenna elements. A need to decoupling structure was necessary to improve the isolation between antennas. Two pairs of vertical and horizontal NLs were printed on the ground plane of MIMO antenna as seen in Fig 2 (b). Each NL printed length is 31 mm and with is 0.3 mm and each line is printed sequentially with the other line on the x and y axis with gap distance 1.8 mm and 3.4 mm for the x and y axis respectively. The parametric study started by increasing the value of D2 from 0.3 to 0.6 mm with a step of 0.15 mm, as seen in Fig. 6. The red curve represents the s-parameters of D2 = 0.3 mm, where it is noted that the antenna resonates at 5.16 GHz with a good enhancement in terms of isolation between elements after print the NLs structure. The value of isolation increased from -13.5 dB to below -19.5 dB with an enhancement value of 6 dB. The obtained improvement is due to printing NLs, which act as conductive elements to reduce electromagnetic coupling between antenna elements. Next, the green curve represents the result when D2 = 0.45 mm which shows the matching impedance and operating bandwidth decreased to operate from 4.95 - 5.19 GHz with increased isolation below -21.5 dB. However, operating bandwidth and matching impedance are important parameters in MIMO antennas. Therefore, value of D2 = 0.3 mm is the perfect value for this parametric study.

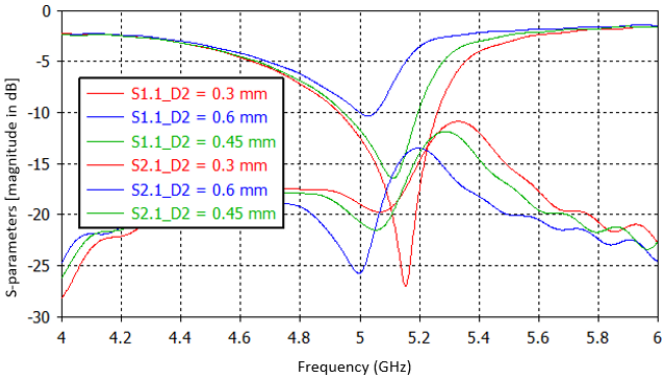


Fig. 6. S-parameter results of changing width of NLs.

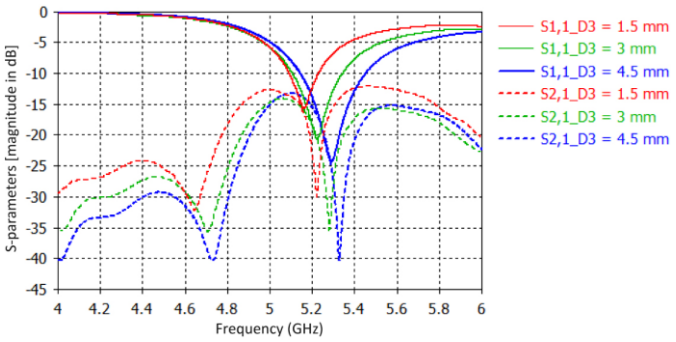


Fig. 7. S-parameter results of changing the length of the etched slot on the ground plane.

Next, to evaluate the effectiveness of the DGS, etch a slot on the center of the ground plane to investigate what the effects are on the MIMO antenna system performance. The D5 parameter represents the value of the etched slot. In this parametric study, the value of D5 will change from 1.5 to 4.5 mm with a step of 1.5 mm. Fig 7(a) and (b) illustrate the s-parameter results (S11 and S21) of the applied investigation. The red curve demonstrates the results when D5 =1.5 mm, as shown in the MIMO antenna operating at 5.16 GHz with an operating bandwidth of 5.8-5.27 GHz and the maximum achieved impedance matching below -17.8 dB. On the other hand, the obtained S21 for the same value was below -17 dB at resonance frequency. The green curve represents the result when D5 = 3 mm, the reflection coefficient in the step shows an improvement in terms of matching impedance and the operating frequency shifted toward operating at 5.23 GHz with matching impedance below -22 dB, In addition, isolation also improved below -21 dB at 5.23 GHz and the maximum achieved isolation is -35 dB. Next, the blue curve illustrates results when D5 = 4.5 mm, the operating frequency shifted toward being operated at 5.29 GHz with maximum matching impedance below -24 dB. In addition, there is a good achievement in terms of isolation below -26 dB at 5.29 GHz and maximum isolation was below -40 dB. The etched slots enhance isolation due to several physical mechanisms. First, the slot disrupts and redistributes the surface current on the ground plane, preventing direct current flow

between adjacent antenna elements. The results confirmed that the inclusion of the DGS significantly improved isolation and contributed to better impedance matching, thus enhancing the overall performance of the MIMO antenna system.

IV. MIMO Performance

To evaluate the effectiveness of the hybrid isolation technique, which combines Defected Ground Structure (DGS) and Neutralization Lines (NLs), a comparative analysis was performed on the MIMO antenna's performance before and after applying the technique. As illustrated in Figure 8, the reference antenna without any isolation enhancements operates at 5.2 GHz with a reflection coefficient (S11) better than −20 dB, indicating good impedance matching. However, the transmission coefficient (S21) shows a relatively poor isolation level of −13.5 dB, and the antenna covers an operational bandwidth from 5.38 to 5.8 GHz. After implementing the hybrid technique, a significant improvement is observed. The antenna operates at a slightly shifted center frequency of 5.29 GHz and achieves an enhanced isolation level below −26 dB across the band, with a minimum isolation reaching below −40 dB at certain frequencies. Additionally, the operational bandwidth is extended and shifted to cover the range from 5.3 to 5.48 GHz. These results demonstrate that the integration of DGS and NLs effectively suppresses mutual coupling between antenna elements and improves isolation without compromising the impedance matching or bandwidth. Therefore, the hybrid approach proves to be a promising technique for enhancing MIMO antenna performance in compact wireless systems.

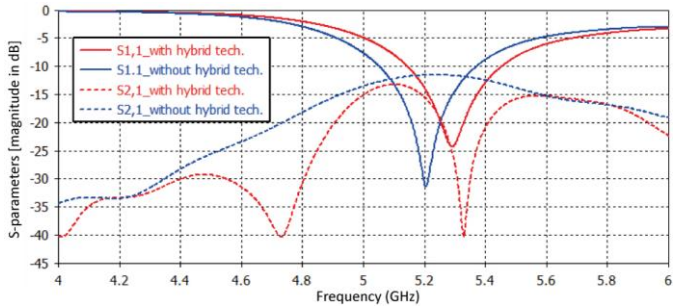
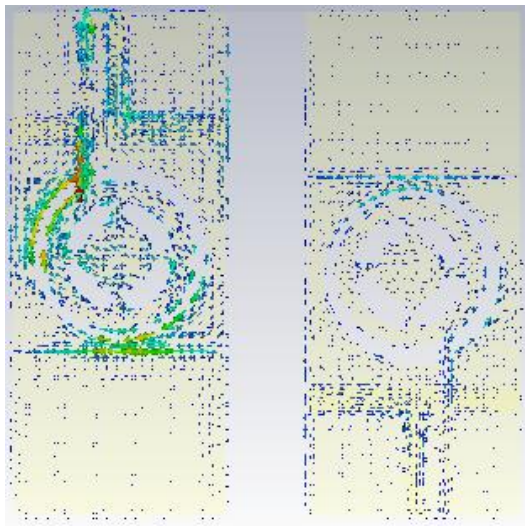


Fig. 8. S-parameter results with and without the proposed hybrid isolated technique.

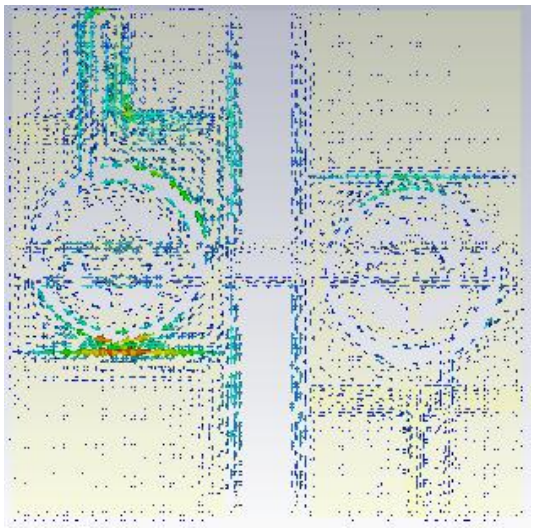
Fig. 9 demonstrates the effect of the hybrid isolation technique in reducing mutual coupling between antenna elements. In the left image (before applying DGS and NLs), a strong current concentration is observed not only on the excited element but also on the adjacent element, indicating significant electromagnetic coupling. This undesired coupling results in degraded isolation performance and can negatively affect the overall MIMO system behavior.

In contrast, the right image (after implementing the hybrid technique) shows a notable reduction in surface current on the adjacent element. The current is more confined around the excited patch and its immediate ground area, which reflects the role of DGS in disrupting surface wave propagation and the NL in introducing a coupling-cancellation path. The current paths appear more controlled and isolated, indicating the suppression of mutual interactions between the elements.

This visual evidence supports the S-parameter results previously discussed, confirming that the combination of DGS and NLs effectively reduces mutual coupling, enhances isolation (to below −40 dB), and improves the electromagnetic compatibility of the MIMO antenna system.



(a)



(b)

Fig. 9. Surface current distribution: a) before and b) after the hybrid isolation technique.

V. Fabrication and Measurement

In this section, the performance of the proposed slot MIMO antenna is validated through fabrication and experimental measurements. A prototype of the antenna, incorporating the hybrid isolation technique to achieve high isolation, was fabricated. The fabricated prototype is shown in Fig 10.

S-parameters: After performing calibration using the vector network analyzer (R3767CG), the reflection and transmission coefficients of the proposed antenna were measured. Fig. 11 (a) illustrates a comparison between the measured and simulated

reflection coefficients. The results indicate that the proposed slot antenna achieves an impedance bandwidth (S11 < –10 dB) that shows good agreement between simulation and measurement. Minor discrepancies between the measured and simulated results can be attributed to imperfections in the feeding mechanism and fabrication process.

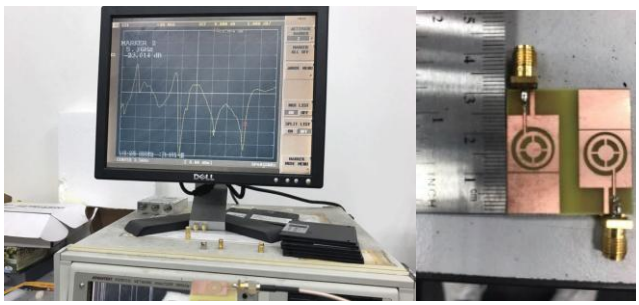
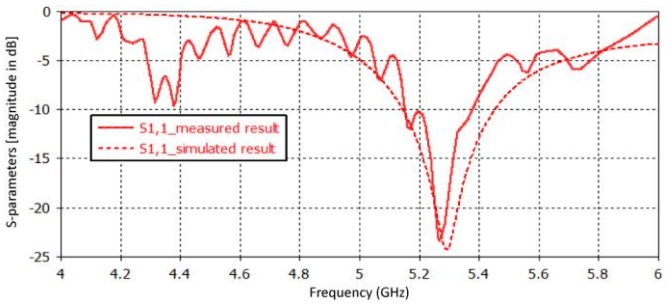
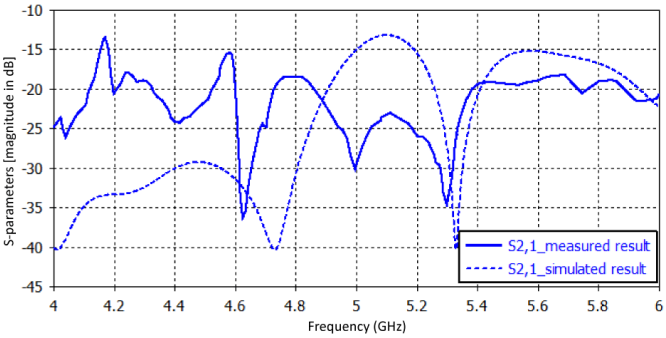


Fig. 10. Prototype of plus-shaped slot MIMO antenna.



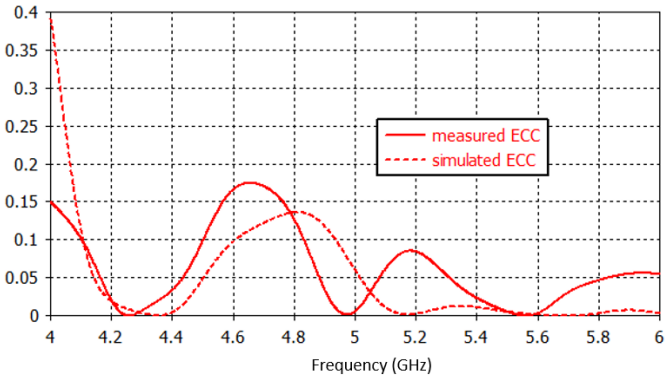
(a)



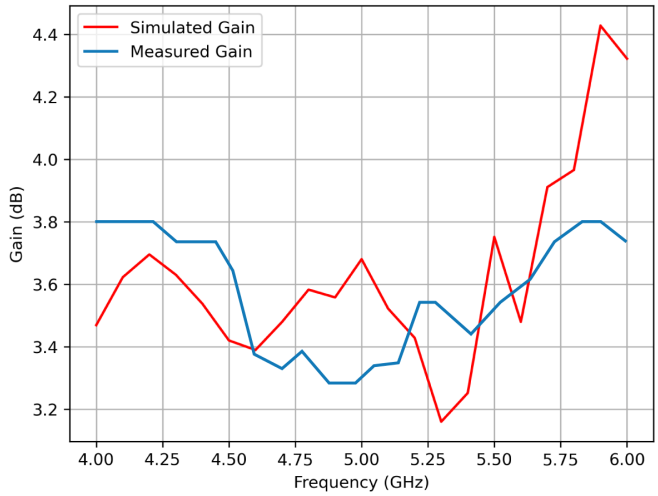
(b)

Fig. 11. Simulated and measured s-parameter results: a) reflection coefficient, b) transmission coefficient.

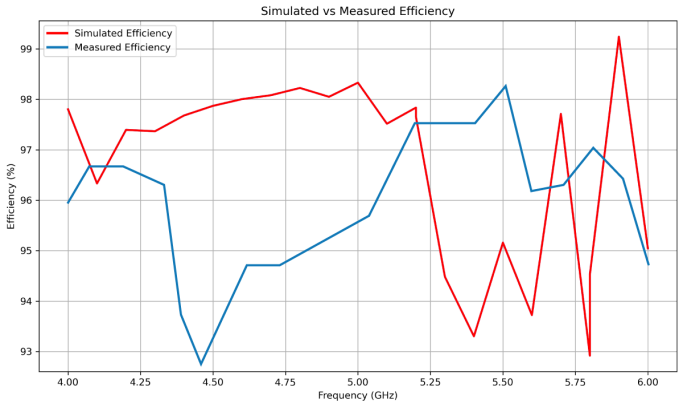
The proposed MIMO antenna resonates at 5.29 GHz and operates over a bandwidth range from 5.14 to 5.39 GHz, maintaining a return loss below –10 dB throughout this frequency band. Figure 11(b) demonstrates a comparison between the simulated and measured transmission coefficient of the proposed slot MIMO antenna. The results show some of the differences between the simulated and measured results due to fabrication errors. However, there is a good similarity between them over the operating bandwidth. The obtained measurement results show that there is a high isolation between antenna elements below -35 dB at 5.29 GHz compared with simulated results which is below -40 dB at the resonance frequency.



(a)



(b)

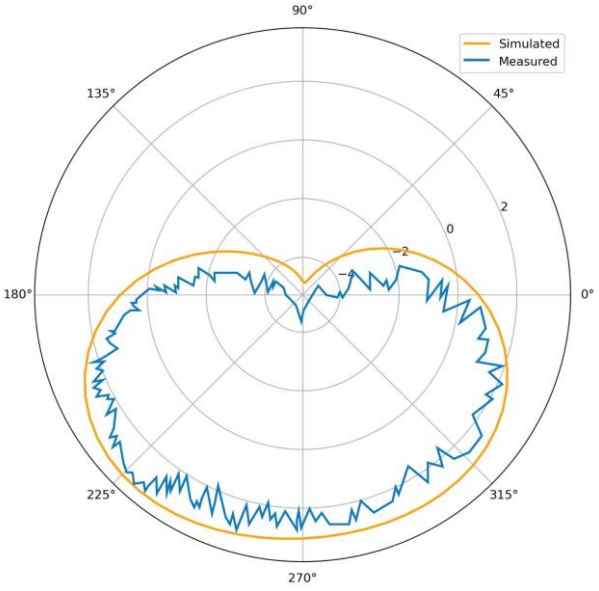


(c)

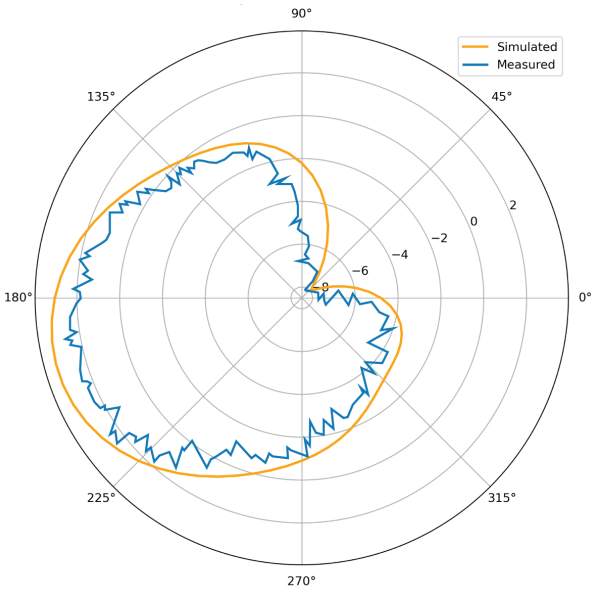
Envelop correlation coefficient (ECC): Since the better operation of the MIMO antennas can be obtained from the incorporation of the ECC in them, this parameter can be calculated from the S-parameter method. From the measured and simulated S-parameters, as shown in Fig. 12(a). The results of ECC in both simulated and prototype environments are compatible and confirm the existence of a lower ECC between the two adjacent antenna elements.

Gain: Fig. 12 (b) illustrates the comparison between the findings of simulated and measured gain for the presented antenna design, which was carried out inside an anechoic chamber. The simulated results show that the antenna obtained a maximum gain of 3.7 dBi at 5 GHz. These results suggest

good radiation characteristics and stable performance across operating frequencies. The measured results show a slightly different trend. Maximum measured gain achieved was 3.57 dBi at 5.2 GHz. In general, the gain ranges between 3.2-3.57 dBi over the operating frequency bandwidth. notes that there are some differences between the simulated and measured results due to the same reasons mentioned above.



(d)



(e)

Fig. 12. Simulated and measured results of: a) ECC, b) Gain, C) Efficiency (d) Radiation pattern Phi = 0 and (e) Radiation pattern Phi = 90.

Radiation Efficiency: Fig. 12(c) presents an analysis of radiation efficiency across the operating frequency range of 5.14–5.39 GHz, showing a generally strong correlation between simulated and measured results. The simulated data indicates radiation efficiency values between 93% and 97%, reflecting a well-optimized antenna design with minimal simulated losses. In contrast, the measured efficiency ranges from 84% to 95%, exhibiting slight deviations from the simulated values. Nonetheless, the measured performance remains high and follows the same overall trend. These differences are likely due to practical factors such as fabrication tolerances, variations in material properties, limitations in the measurement setup, and losses from connectors or cables factors typically not included in ideal simulation models.

Figures 12 (d) and (e) show ripples in measured radiation patterns, which are mainly attributed to practical measurement progress. Because of that, some reflections from surrounding objects and imperfections in the measurement environment, in return cause constructive and destructive interference. Figs 12 (d and e) demonstrate the simulation and measured radiation patterns of the proposed slot MIMO antenna. In general, the results show a good agreement between the simulated and measured results, which confirm the validating antenna fabrication. As seen from the reported results, the peak radiation occurs approximately around 180°–270°, indicating a directional pattern, depending on the cut.

VI. Comparison with Previous Studies

TABLE II
Comparisons between the Proposed Plus-shaped MIMO Antenna and Previous Related Antennas.

Ref.	Size (mm^3)	Iso. (dB)	BW (dB)	Iso. Tech.	Dis. (mm)
[7]	30×60×1.6	-21	3–12	EBG	15
[8]	48×48×1.6	-10.5	3.3–3.7	EBG	Not mentioned
[9]	40×40×1.6	-15	3.2-5.75	DGS	4
[10]	100×50×0.8	-25	5.2-6	DGS	Not mentioned
[11]	Not mentioned	-23	3.4-3.6	DN	11.5
[12]	60×60×1.6	-15	4.52–5.56	DN & NL	5
[13]	21.5×28×1.6	-16	3.4-12.1	NL	3.8
[14]	30×18×1.6	-15	4.3–15.63	DN	10
[15]	37×37×0.508	-29	5.53–7.32	DN	7
[16]	64×36×0.8	-15	3.7 - 4.3	PE	36.85
[17]	60 x50 x1.6,	-12	5.8-5.95	NL	10
[18]	27× 28×0.787	-35	5.15-5.35	EBG	Not mentioned
[19]	12.5×37×0.8	-16.5	3.3-3.7	NL & DGS	3
Proposed slot antenna	31×31×1.6	-35	5.17-5.47	NL & DGS	4

Table II provides a comparative analysis between the proposed wideband MIMO antenna and several selected designs from existing literature. The selection criteria for the comparative study include compact antenna size, high isolation, wide bandwidth, low envelope correlation coefficient (ECC), the type of isolation technique employed, and the distance between antenna elements. The comparison reveals that the proposed antenna offers superior isolation performance while maintaining a more compact size, highlighting its effectiveness and suitability for modern wireless communication systems.

VII. Conclusion

A two ports MIMO antenna with compact size and distance has been presented. The hybrid isolation technique consisting of DGS and NLs was the perfect choice to achieve a high isolation between antenna elements. The proposed MIMO antenna has been fabricated on FR-4 substrate with a thickness of 1.6 mm. The results show that the presented MIMO antenna operates from 5.17 to 5.47 GHz, while the obtained ECC is 0.026. The main contribution of this study is achieving high isolation of -35 dB corresponding to an enhancement of approximately 169% with small distance and compact size. Radiation efficiency and gain were also investigated and showing the radiation efficiency ranging between 93% and 97% while the gain ranged between 3.2 and 3.57 dBi. Depending on the achieved results, the presented MIMO antenna has a good performance and it is suitable for the modern system of 5G communication.

References

[1] H. Islam et al., "Compact circularly polarized 2 and 4 port multiple input multiple output antennas with bandstop filter isolation technique," Alexandria Eng. J., vol. 66, pp. 357–376, 2023, doi: 10.1016/j.aej.2022.11.029.

[2] V. Tashvigh and M. Kartal, "International journal of electronics and communications regular paper a dual-sense CP MIMO antenna using decoupling structure with improved isolation," AEU - Int. J. Electron. Commun., vol. 175, Art. no. 155065, 2024, doi: 10.1016/j.aeue.2023.155065.

[3] Mamta and V. Nath, "L-shaped reconfigurable band decoupling assisted dual band four port MIMO antenna for 5G and IoT application," AEU - Int. J. Electron. Commun., vol. 179, Art. no. 155295, 2024, doi: 10.1016/j.aeue.2024.155295.

[4] M. Saxena, "Neutralized line and slot loaded compact MIMO antenna for WLAN applications," in Proc. 2024 IEEE 11th Uttar Pradesh Sect. Int. Conf. Electr. Electron. Comput. Eng., 2024, pp. 1–4, doi: 10.1109/UPCON62832.2024.10983808.

[5] A. Ali, M. E. Munir, M. M. Nasralla, M. A. Esmail, A. J. A. Al-Gburi, and F. A. Bhatti, "Design process of a compact tri-band MIMO antenna with wideband characteristics for sub-6 GHz, Ku-band, and millimeter-wave applications," Ain Shams Eng. J., vol. 15, no. 3, Art. no. 102579, 2024, doi: 10.1016/j.asej.2023.102579.

[6] P. Kumar et al., "Results in engineering a quad port dual band notch UWB MIMO antenna using hybrid decoupling structure," Results Eng., vol. 23, Art. no. 102551, 2024, doi: 10.1016/j.rineng.2024.102551.

[7] N. S. Babu, A. Q. Ansari, B. K. Kanaujia, G. Singh, and S. Kumar, "A two-port UWB MIMO antenna with an EBG structure for WLAN/ISM applications," Mater. Today Proc., vol. 74, pp. 334–339, 2023, doi: 10.1016/j.matpr.2022.08.316.

[8] G. Tamminaina and R. Manikonda, "Investigation on performance of four port MIMO antenna using electromagnetic band gap for 5G communication," Prog. Electromagn. Res. M, vol. 119, pp. 51–62, 2023, doi: 10.2528/PIERM23080303.

[9] C. Güler and S. E. Bayer Keskin, "A novel high isolation 4-port compact MIMO antenna with DGS for 5G applications," Micromachines, vol. 14, no. 7, Art. no. 1309, 2023, doi: 10.3390/mi14071309.

[10] P. Kumar, T. Ali, S. Pathan, N. Kumar Shetty, Y. Bommenahalli Huchegowda, and Y. Nanjappa, "Design and analysis of ultra-wideband four-port MIMO antenna with DGS as decoupling structure for THz applications," Results Opt., vol. 13, Art. no. 100573, 2023, doi: 10.1016/j.rio.2023.100573.

[11] G. Zhao et al., "A three-port coupled resonator decoupling network for mutual coupling reduction of three-element antenna arrays," IEEE Trans. Microw. Theory Tech., vol. 72, no. 11, pp. 6585–6600, 2024, doi: 10.1109/TMTT.2024.3400120.

[12] X. J. Zou et al., "Wideband coupling suppression with neutralization-line-incorporated decoupling network in MIMO arrays," AEU - Int. J. Electron. Commun., vol. 167, Art. no. 154688, 2023, doi: 10.1016/j.aeue.2023.154688.

[13] D. Saxena, A. Kumar, R. K. Verma, and P. Jha, "Metamaterial inspired dual band MIMO antenna with open-ended slot and neutralized line for isolation enhancement," in Proc. 10th Int. Conf. Signal Process. Integr. Networks (SPIN), vol. 2, 2023, pp. 727–732, doi: 10.1109/SPIN57001.2023.10117256.

[14] I. A. T. K, A. K. A, S. Mathew, and R. K, "Computer vision-based location-aware antenna system for 5G applications," e-Prime - Adv. Electr. Eng. Electron. Energy, vol. 12, Art. no. 101004, 2025, doi: 10.1016/j.prime.2025.101004.

[15] H. Elmannai et al., "Design and characterization of a meandered V-shaped antenna using characteristics mode analysis and its MIMO configuration for future mmWave devices," AEU - Int. J. Electron. Commun., vol. 186, Art. no. 155477, 2024, doi: 10.1016/j.aeue.2024.155477.

[16] H. H. Tran, T. T. L. Nguyen, H. N. Ta, and D. P. Pham, "A metasurface-based MIMO antenna with compact, wideband, and high isolation characteristics for sub-6 GHz 5G applications," IEEE Access, vol. 11, pp. 67737–67744, 2023, doi: 10.1109/ACCESS.2023.3292303.

[17] H. Chen, H. Kim, Y. Liu, Y. Liu, and L. Qu, "Compact quarter-mode SIW MIMO antennas using neutralization line for V2X applications," in Proc. 2024 Int. Appl. Comput. Electromagn. Soc. Symp. (ACES-China), 2024, pp. 1–3, doi: 10.1109/ACES-China62474.2024.10699619.

[18] Y. Tang, T. Wang, J. Zheng, Z. Lyu, X. Tian, and J. Mou, "Mutual coupling suppression of MIMO array with non-uniform curved-strip EBG structure via shape and layout co-optimization," AEU - Int. J. Electron. Commun., vol. 178, Art. no. 155306, 2024, doi: 10.1016/j.aeue.2024.155306.

[19] P. Kumar et al., "A quad port dual band notch UWB MIMO antenna using hybrid decoupling structure," Results Eng., vol. 23, Art. no. 102551, 2024, doi: 10.1016/j.rineng.2024.102551.



Mohammed Abdulwahab Khary received the Bachelor Degree in Computer techniques engineering from Dijlah University, Iraq, in 2011 and Master in Nano electronics from Mordovia national university, Russia in 2018. Now, he is an assistant lecturer at AlFarahidi University.



Ahmed Raed Al-Tameemi received the Bachelor Degree in Computer techniques engineering from Dijlah University, Iraq, in 2011 and Master in Nano electronics from Mordovia National University, Russia in 2018. He is Assistant lecturer with the Department of Computer Techniques Engineering, Al-Nisour University. In the same time, He is manager of IT department in Al-Nisour University. His work and research interest includes, utility communication technology, electromagnetic technology.



Goh Chin Hock received the Bachelor Degree in Electrical and Electronics Engineering in 2004 as well as Master and PhD in Electrical Engineering in 2008 and 2012 respectively from Universiti Tenaga Nasional, Malaysia. He is currently an Associate Professor with the Department of Electrical and Electronics Engineering, Universiti Tenaga Nasional. He is the Professional Engineer of BEM, Energy Professional of MEPA and Corporate Member of IEM. Besides that, he is Certified Energy Manager (CEM), Certified Professional in Measurement and Verification (CPMV) as well as Registered Electrical Energy Manager (REEM). His work and



Sieh Kiong Tiong received the B.Eng. (Hons.), M.Sc., and Ph.D. degrees in electrical, electronics and system engineering from the National University of Malaysia (UKM), in 1997, 2000, and 2006, respectively. He is currently a Professor with the College of Engineering, Universiti Tenaga Nasional, where he is also the Director of the Institute of Sustainable Energy (ISE). His research interests include renewable energy, artificial intelligence, data analytics, microcontroller systems, and communication systems. He is currently a Professional Engineer registered with the Board of Engineers Malaysia (BEM).



Taha Al Sheikhly is an Iraqi academic specializing in computer and telecommunications engineering at the University of Technology. He holds a Ph.D. in electronics and computer engineering from Universiti Teknikal Malaysia Melaka and conducts research in antennas, wireless communications, MIMO systems, and advanced electromagnetic applications, including lightning detection technologies. He has contributed to several scientific publications and collaborates on research in modern communication systems and nanoelectronics.



Assim Mudhafar Fadhil is a researcher in the field of physics and renewable energy, affiliated with the School of Applied Physics at Universiti Kebangsaan Malaysia. His work focuses on experimental and computational physics, with particular emphasis on solid-state physics, photovoltaic systems, and sustainable energy technologies. He has contributed to research on desalination systems powered by renewable energy, especially photovoltaic-driven reverse osmosis for brackish water treatment, aiming to develop efficient and cost-effective solutions for water production in remote areas. His research also explores modeling, simulation, and optimization techniques to enhance system performance, alongside ongoing work in advanced materials such as graphene oxide.